Research Square

Preprints are preliminary reports that have not undergone peer review.
They should not be considered conclusive, used to inform clinical practice,
or referenced by the media as validated information.

A tumoral and peritumoral CT-based Radiomics and Machine learning approach to predict the microsatellite instability of rectal carcinoma

Yanqing Ma (704180026@qq.com)
Zhejiang Provincial People's Hospital, Hangzhou Medical College
Hang Yuan
Zhejiang Provincial People's Hospital, Hangzhou Medical College
Peng Yu
Zhejiang Provincial People's Hospital, Hangzhou Medical College
Xiren Xu
Zhejiang Provincial People's Hospital, Hangzhou Medical College
Shiliang Tu
Zhejiang Provincial People's Hospital, Hangzhou Medical College
Yuguo Wei
Precision Health Institution

Research Article

Keywords: Rectal carcinoma, Microsatellite instability, Computed tomography, Machine learning, Radiomics, Nomogram

Posted Date: February 24th, 2022

DOI: https://doi.org/10.21203/rs.3.rs-1305223/v1

License: This work is licensed under a Creative Commons Attribution 4.0 International License.
Read Full License

Abstract

Objective: To predict the status of microsatellite instability (MSI) of rectal carcinoma (RC) using different machine learning algorithms based on tumoral and peritumoral radiomics combined with clinicopathological characteristics.

Methods: There were 487 RC patients enrolled in this retrospective study. The tumoral and peritumoral CT-based radiomic features were calculated after tumor segmentation. The radiomic features from two radiologists were compared by the method of inter-observer correlation coefficient (ICC). After methods of variance, correlation, and dimension reduction, six machine learning algorithms of logistic regression (LR), Bayes, support vector machine, random forest, k-nearest neighbor, and decision tree were conducted to develop models in predicting MSI status of RC. The relative standard deviation (RSD) was quantified. The radiomics and significant clinicopathological variables were integrated the radiomics-clinicopathological nomogram. The receiver operator curve (ROC) was made by Delong test and the area under curve (AUC) with 95% confidence interval (95%CI) was calculated to evaluate the performance of the model.

Results: The venous phase of CT examination was selected for further analysis because of the proportion of radiomic features with ICC greater than 0.75 was higher. The tumoral and peritumoral model by LR algorithm (M-LR) with minimal RSD showed good performance in predicting MSI status of RC with the AUCs of 0.817 and 0.726 in the training and validation set. The radiomic-clinicopathological nomogram conducted better in both the training and validation set with the AUCs of 0.843 and 0.737.

Conclusion: The radiomics-clinicopathological nomogram demonstrated the better predictive performance in evaluating the MSI status of RC.

Background

Rectal carcinoma (RC) is the third most frequent malignancy worldwide with significant difference between clinical characteristics, prognosis, and individual treatment response[1]. Preoperative chemotherapy is the recommended therapy for patients with resectable advanced RC with the advantages of down-staging, enhancing the rate of curative surgeries and permitting sphincter preservation in patients with low-lying tumors[2]. Microsatellite instability (MSI) is an important biomarker to predict the response of chemotherapy and clinical outcomes of RC, which is always tested by immunohistochemistry displaying loss of one or more mismatch repair (MMR) proteins[3]. Whereas, tumors with intact MMR proteins were collectively referred as microsatellite stability (MSS) status[4]. Patients with MSI status obtained no benefit from adjuvant treatment with 5-fluorouracil and had better prognosis than patients with MSS[5]. Therefore it is important to develop a noninvasive and reproducible approach to identify the MSI status of rectal carcinoma[6].

Radiomics is considered as a high throughput method to convert the conventional medical images into quantitative radiomics features[7], and is gaining increasing attention in cancer-related research[8]. Previous publication using the CT-based radiomics method reported that radiomics features combined clinical features helped to evaluated the MSI status of colorectal carcinoma[9]. As the clinical-radiomics nomogram illustrated that radiomics features, tumor location, age, high-density lipoprotein expression, and platelet counts showed good performance in assessing MSI status of colorectal cancer[10].

To best of our knowledge, there was no tumoral and peritumoral radiomics based machine learning study in predicting MSI status of RC patients. In this article, we developed a machine learning model with tumoral and peritumoral CT radiomics features to identify MSI status of RC.

Materials And Methods

Patients enrollment

This study was conducted with the permission of the institutional review board of our hospital (No. 2021QT339). The individual informed consent was waived for this retrospective study. Between January 2017 and January 2021, there were 497 patients whom were pathologically confirmed as RC were enrolled. The patients who underwent preoperative CT examinations within two weeks before surgeries, were confirmed as the type of classical adenocarcinoma of RC, didn't received preoperative chemotherapy or chemoradiotherapy, were not accompanied with other cancer, and were taken MSI testing were chosen. The flow-chat of patients enrollment was listed in Fig. 1. Finally, 497 RC patients including 96 patients with MSI status and 401 patients with MSS status were retrospectively selected in this study.

CT examination

All the patients underwent triphasic CT examinations on a 64 slices (127 patients) or 128 slices (370 patients) CT scanner (Somaton Definition AS, Siemens, Germany) including unenhanced phase, arterial phase, and venous phase. The triphasic CT scanning was conducted after injecting a does of 1.3 mL/Kg contrast media (iomeperol 350) at a a rate of 3.0 mL/s. Then the arterial phase and venous phase were scanned after 15 seconds and 30 seconds of unenhanced phase. The uniform parameters were as follows: tube voltage 120 Kv, tube current 200mA, field of view 360mm, rotation time 0.75s, collimation 64*0.625mm, interval thickness 5mm.

Evaluation the clinicopathological characteristics and MSI status

The clinicopathological characteristics of RC patients comprised age, gender, CT-displayed diameter, location, carcinoembryonic antigen (CEA), carbohydrate 19 – 9 (CA19-9), lymph node metastasis ratio (LNR, LNR = positive lymph node count/lymph node count*100%), perineural invasion (PNI), extramural

venous invasion (EMVI), the history of smoking, drinking, diabetes, and hypertension. The tumor location was divided into low-lying which referred to the lesion located within 5cm from anal margin, middle-lying which referred to the lesion located between 5cm to 10cm from anal margin, and high-lying which referred to the lesion located more than 10cm from anal margin. And the tumor located in the rectosigmoid junction was classified as high-lying RC. The threshold values of CEA and CA19-9 were 5.0 ng/mL and 37.0 U/mL. When the tumor histopathologically invaded the surrounding tissues including perineural structure[11] and extramural venous[12] was defined as PNI and EMVI. The MSI status was assessed by the method of immunohistochemistry to test MMR proteins including MLH1, MSH2, MSH6, and PMS2. Then the RC patients were divided into MSI and MSS group based on whether they were deficient in one or more MMR proteins.

Tumor segmentation and radiomic features selection

The process of tumor segmentation was divided into three steps: (1) before tumor segmentation, the DICOM images were reconstructed into the voxel of 1.0 in X/Y/Z axes and the gray scale into 1 to 32 in A.K. software (Artificial Intelligence Kit, GE Healthcare) for standardization, automatically. (2) the tumoral volume of interest (VOI-t) was depicted in itk-SNAP software (Version 3.4.0. https://www.itksnap.org/) by two radiologists with about 10 years of diagnostic experience, manually (Fig. 2a). (3) the peritumoral VOI (VOI-pt) was acquired after expanding 5mm from the VOI-t in A.K. software, automatically (Fig. 2b). The regions of intraluminal air, peritumoral structures including bone, bowl, prostate, and uterus were eliminated from the contours of VOI-pt.

The selection of radiomic features was divided into four steps: (1) after the segmentation of VOI-t and VOI-pt, the radiomics features were calculated in A.K. software, automatically. (2) the radiomic features from two radiologists were compared by the method of inter-observer correlation coefficient (ICC). And ICC greater than 0.75 is considered to be of good reliability and accuracy. So the phase with more radiomic features with ICC greater than 0.75 was chosen for analyze. (3) the cohort was randomly assigned into the training set and validation set with a proportion of 7:3. (4) the dimension reduction of radiomic features was performed by the method of pre-processing, variance, correlation analysis, and least absolute shrinkage and selection operator (LASSO). Specific information was reported in Supplementary Materials.

Radiomics-based machine learning

After the selection of radiomic features, six machine learning algorithms including logistic regression (LR), Bayes, support vector machine (SVM), random forest (RF), k-nearest neighbor (KNN), and decision tree (DT) were conducted to construct radiomics models. The 100 Bootstrap replication and its relative standard deviation (RSD) was taken to quantify the stability of six algorithms. The equation of RSD was: (the standard deviation of the 100 AUC values of each machine learning algorithm)/(the corresponding mean value of the 100 AUC values)*100%[13]. The lower the RSD value, the higher the stability of the algorithm. Therefore the algorithm with minimal RSD value was selected for further analysis. Finally, the

radiomics score (Rad-score) was calculated to quantify the radiomics-based machine learning algorithm in predicting the MSI status of RC.

Integration of radiomics and clinicopathological characteristics analysis

The method of multivariate logistic regression of backward stepwise selection was used to analyze the integration of radiomic features and significant clinicopathological characteristic, and the integrative model was built. The receiver operator curve (ROC) was made by Delong test and the area under curve (AUC) with 95% confidence interval (95%CI) was calculated to evaluate the performance of the model. The Hosmer-Lemeshow test was taken to evaluate the goodness-of-fit and accuracy of the model.

Statistical analysis

All statistical analysis for the radiomic features selection and machine learning algorithm were performed in R software (Version 3.5.1, https://www.r-project.org/) and Python (Version 3.5.6, https://www.python.org/). The methods to analyze the clinicopathological characteristics including independent t-test and Pearson chi-square test were implemented in SPSS software (Version 22, https://spss-64bits.en.softonic.com/). The Delong test and ROC were carried out in MedCalc software (Version 18.2, https://www.medcalc.org/). A two-tailed p value < 0.05 indicated statistical significance.

Results

General clinicopathological characteristics

The clinicopathological characteristics of gender, age, CT-displayed diameter, location, CA19-9, PNI, EMVI, history of smoking, drinking, diabetes, and hypertension were not statistically different (p = 0.054–0.768). While, statistical difference was noted in clinicopathological variables of CEA (p = 0.007), LNR (p = 0.003), and history of drinking (p = 0.016). The specific data of clinicopathological characteristics was shown in Table 1.

Table 1
The characteristics of RC patients with MSI and MSS status.

	MSI status (n = 96)	MSS status (n = 401)	*p* value
Age (years, SD)	64.23 (10.82)	63.30 (11.24)	0.464
Gender (female, %)	32 (33.33%)	149 (37.16%)	0.484
CT-displayed diameter (mm, SD)	3.80 (1.50)	3.75 (1.46)	0.768
Location			0.675
Low-lying (n, %)	22 (22.92%)	91 (22.69%)	
Middle-lying (n, %)	41 (42.71%)	154 (38.40%)	
High-lying (n, %)	33 (34.38%)	156 (38.90%)	
CEA (ng/mL)	4.35 (4.82)	15.27 (79.33)	0.007*
CA19–9 (U/mL)	50.17 (242.60)	32.60 (120.22)	0.492
Smoking (n, %)	27 (28.13%)	77 (19.20%)	0.054
Drinking (n, %)	23 (23.96%)	56 (13.97%)	0.016*
Diabetes (n, %)	10 (10.42%)	49 (12.22%)	0.624
Hypertension (n, %)	41 (42.71%)	136 (33.92%)	0.106
LNR (mean, SD)	4.42 (9.59)	8.29 (16.11)	0.003*
PNI (n, %)	28 (29.17%)	110 (27.43%)	0.733
EMVI (n, %)	39 (40.63%)	174 (43.39%)	0.623

Note. MSI status, RC patients with the status of microsatellite instability; MSS status, RC patients with the status of microsatellite stability; CEA, carcinoembryonic antigen; CA19-9, carbohydrate 19 – 9; LNR, lymph node metastasis ratio; PNI, perineural invasion; EMVI, extramural venous invasion.

Radiomics and machine learning analysis

After the method of ICC between radiomic features from two radiologists, there were 72.3% radiomic features with ICC greater than 0.75 in venous phase compared with 60.1% in unenhanced phase and 69.4% in arterial phase. Therefore we chosen the venous phase and the mean values of radiomic features from two radiologists were calculated for further analysis. The cohort of 497 RC patients were separated into the training set (67 MSI and 281 MSS) and validation set (29 MSI and 120 MSS) with a proportion of 7:3.

Of the 792 tumor and peritumoral radiomic features, 51 radiomic features including 19 tumoral and 32 peritumoral radiomic features were selected after methods of dimension reduction. The LASSO path plot in the training set was illustrated in Fig. 3. These features were listed in the Supplementary Materials. After the method of 100 Bootstrap replication, the RSD of six machine learning algorithm was quantified. The RSD value (mean ± SD) of LR (3.05%, 0.820 ± 0.025) was the minimum compared with that of Bayes (3.10%, 0.773 ± 0.024), SVM (27.95%, 0.755 ± 0.211), RF (7.26%, 0.895 ± 0.065), KNN (4.68%, 0.727 ± 0.034), and DT (8.20%, 0.610 ± 0.050). Hence, we selected the machine learning algorithm of LR to construct tumoral and peritumoral radiomics model (M-LR). The AUCs of M-LR in the training set and validation set (Fig. 4a,b) were 0.817 (95%CI, 0.772–0.856) and 0.726 (95%CI, 0.648–0.796). The equation of M-LR and specific information was listed in Supplementary Material and the Rad-score was calculated.

Performance of radiomics-clinicopathological nomogram

The significant clinicopathological characteristics of CEA ($p = 0.007$), LNR ($p = 0.003$), and drinking history ($p = 0.016$) combined with Rad-score developed a visual nomogram to evaluated the MSI status of RC patients (Fig. 5).The calibration curves of this integrative model demonstrated a good agreement with the ideal curve in both the training set and the validation set which were illustrated in Supplementary Material. The non-significant Hosmer-Lemeshow test ($X^2 = 6.178$, df = 8, $p = 0.627$) indicated the goodness-of-fit of the radiomics-clinicopathological model in evaluate the MSI status of RC patients. Moreover, this integrative model perform better with the AUC of 0.843 (95%CI, 0.800–0.880) in the training set and with the AUC of 0.737 (95%CI, 0.659–0.805) in the validation set (Fig. 4a,b).

Discussion

We selected the venous phase of CT examination for analysis after comparing the ratio of ICC greater than 0.75 of radiomic features from two radiologists in three phases (72.3% of venous phase vs. 60.1% of unenhanced phase and 69.4% of arterial phase). Existing research has suggested that the venous phase was superior compared with arterial phase for lymph node assessment and the arterial phase was better for local tumor staging[14]. We chose the venous phase to analyze the MSI status of RC patients. According the guidelines of National Comprehensive Cancer Network, patients with MSI status have a better prognosis and obtain no benefit from 5-FU-based adjuvant chemotherapy in stage II colorectal carcinoma[15]. Therefore, it is significant to noninvasively and preoperatively predict the MSI status of RC patients. Recent developments in the field of radiomics have reported that combining radiomics with clinical factors could achieve a better predictive performance in predicting MSI status of patients with stage II colorectal carcinoma[16]. While ,to best of our knowledge, there was no research focused on the tumoral and peritumoral radiomics to evaluate the MSI status of RC patients.

We conducted tumoral and peritumoral CT-based radiomics analysis and developed six machine learning algorithms to predict the MSI status of RC patients. We taken the indicator of RSD of 100 Bootstrap replication to assess the different performance of algorithms. The lower the RSD value of the algorithm was, the more stable its performance is. So we selected the algorithm of LR (RSD: 3.05%) to construct a

integrative model of tumoral and peritumoral radiomics to assess the MSI status of RC patients compared with the algorithms of Bayes (RSD: 3.10%), SVM (RSD: 27.95%), RF (RSD: 7.26%), KNN (RSD: 4.68%), and DT (RSD: 8.20%). After the dimension reduction of radiomic features, there were 51 radiomic features remained to construct the M-LR. The AUCs of M-LR were 0.817 (95%CI, 0.772–0.856) in the training set and 0.726 (95%CI, 0.648–0.796). The MRI-based radiomics and machine learning showed that the Bayes-based radiomics signature performed better compared with other LR-based, SVM-based, KNN-based, and RF-based radiomics signature to predict the extramural venous invasion in RC patients[17]. The deep learning based on high-resolution T2-weighted magnetic resonance images showed a good predictive performance for MSI status in RC patients[18]. The multivariate analysis of previous study to predict the treatment response of RC patients found that RF and KNN achieved the highest AUC among pre-treatment and post-treatment features[19]. In our study, the algorithm of LR with the minimal RSD showed the best performance in predict the MSI status of RC patients.

Previous study indicated that colorectal carcinoma with MSI status have distinct clinicopathological and pathological characteristics compared with these with MSS status, including proximal colon predominance, poor differentiation, and abundant tumor infiltrating lymphocytes[20]. Therefore, we integrated the 51 selected radiomic features and significant clinicopathological variables of CEA, LNR, and drinking to construct a visual nomogram in predicting the MSI status of RC patients. The preoperative prediction of MSI status via CT-based radiomics adds specificity to clinical assessment and could contribute to personalized therapy[9]. The radiomics nomogram incorporating radiomics signatures and clinical indicators of tumor location, patient age, high-density lipoprotein expression, and platelet counts could potentially be used to facilitate the individualized prediction of MSI status in patients with colorectal carcinoma[10]. To best of our knowledge, there was no machine learning research incorporating CT-based radiomics and clinicopathological variables to predict the MSI status of RC. Our integrated radiomics-clinicopathological nomogram showed a better performance with AUCs of 0.843 (95%CI, 0.800–0.880) in the training set and 0.737 (95%CI, 0.659–0.805) in the validation set than the simple M-LR.

Conclusion

The present research explored, for the first time, the effects of CT-based tumoral and peritumoral radiomics with the machine learning algorithm of LR could help predict the MSI status of RC patients. Moreover, the visual radiomics-clinicopathological nomogram incorporating radiomics and significant clinicopathological variables of CEA, LNR, and drinking performed better prediction of MSI status of RC patients .

Abbreviations

Rectal carcinoma: RC

Microsatellite instability: MSI

Mismatch repair: MMR

Microsatellite stable status: MSS

Carcinoembryonic antigen: CEA

Carbohydrate antigen 19-9: CA19-9

Lymph node metastasis ratio: LNR

Perineural invasion: PNI

Extramural venous invasion: EMVI

tumoral volume of interest: VOI-t

Peritumoral volume of interest: VOI-pt

Intraclass correlation coefficient: ICC

least absolute shrinkage and selection operator: LASSO

logistic regression: LR

Support vector machine: SVM

Random forest: RF

k-nearest neighbor: KNN

Decision tree: DT

Relative standard deviation: RSD

The area under curve: AUC

Receiver operator curve: ROC

95% confidence interval: 95%CI

Radiomics model of logistic regression: M-LR

Declarations

Ethics approval and consent to participate:

This retrospective study was approved by the Medical Ethics Committee of Zhejiang Provincial People's Hospital (No. 2021QT339) and in conformity to the Declaration of Helsinki. The informed consent was waived for this retrospective study by the Medical Ethics Committee of Zhejiang Provincial People's Hospital (No. 2021QT339).

Consent for publication:

All the authors agreed the publication in BMC Cancer.

Availability of data and materials:

The datasets used and analyzed in this article is available from the corresponding author on reasonable request. The code used in this study is available at GitHub (https://github.com/mayq1988/MSI).

Competing interests:

No competing interests.

Funding:

The study was supported by the fund of Medical and Health Research Project of Health Commission of Zhejiang Province (No. 2022492695).

Authors' contribution:

Yanqing Ma: Conceptualization, Methodology, Writing-Original Draft. Peng Yu: Writing-Review & Editing, Supervision. Xiren Xu: : Software, Formal analysis, Data Curation. Shiliang Tu: Validation, Resources. Yuguo Wei: Validation, Resources, statistics, and software. Hang Yuan: Conceptualization, Methodology, and editing.

Acknowledgements:

not applicable.

References

1. Mattiuzzi C,Lippi G. Current Cancer Epidemiology[J]. J Epidemiol Glob Health, 2019, 9(4):217-222.

2. Sauer R, Becker H, Hohenberger W, et al. Preoperative versus postoperative chemoradiotherapy for rectal cancer[J]. New England Journal of Medicine, 2004, 351(17):1731-1740.
3. Sinicrope F A,Sargent D J.Molecular pathways: microsatellite instability in colorectal cancer: prognostic, predictive, and therapeutic implications[J]. Clinical Cancer Research, 2012, 18(6):1506-1512.
4. Trojan J, Stintzing S, Haase O, et al. Complete pathological response after neoadjuvant short-course immunotherapy with ipilimumab and nivolumab in locally advanced MSI-H/dMMR rectal cancer[J]. The Oncologist, 2021.
5. Oh C R, Kim J E, Kang J, et al. Prognostic Value of the Microsatellite Instability Status in Patients With Stage II/III Rectal Cancer Following Upfront Surgery[J]. Clin Colorectal Cancer, 2018, 17(4):e679-e685.
6. Kenneth A. Miles M, Balaji Ganeshan B, Matthew R. Griffiths M, et al. Colorectal Cancer: Texture Analysis of Portal Phase Hepatic CT Images as a Potential Marker of Survival[J]. Radiology, 2009, 250(2):444-452.
7. Baeßler B, Weiss K,Santos D P d.Robustness and Reproducibility of Radiomics in Magnetic Resonance Imaging: A Phantom Study[J]. Investigative Radiology, 2018, 54(4):221-228.
8. Gillies R J, Kinahan P E,Hricak H.Radiomics: Images Are More than Pictures, They Are Data[J]. Radiology, 2016, 278(2):563-577.
9. Golia Pernicka J S, Gagniere J, Chakraborty J, et al. Radiomics-based prediction of microsatellite instability in colorectal cancer at initial computed tomography evaluation[J]. Abdom Radiol (NY), 2019, 44(11):3755-3763.
10. Pei Q, Yi X, Chen C, et al. Pre-treatment CT-based radiomics nomogram for predicting microsatellite instability status in colorectal cancer[J]. European Radiology, 2022, 32(1):714-724.
11. Liebig C, Ayala G, Wilks J A, et al. Perineural invasion in cancer: a review of the literature[J]. Cancer, 2009, 115(15):3379-3391.
12. Inoue A, Sheedy S P, Heiken J P, et al. MRI-detected extramural venous invasion of rectal cancer: Multimodality performance and implications at baseline imagingand after neoadjuvant therapy[J]. Insights Imaging, 2021, 12(1):110.
13. Parmar C, Grossmann P, Bussink J, et al. Machine Learning methods for Quantitative Radiomic Biomarkers[J]. Sci Rep, 2015, 5(13087.
14. Hundt W, Braunschweig R,Reiser M.Evaluation of spiral CT in staging of colon and rectum carcinoma[J]. European Radiology, 1999, 9(1):78-84.
15. Piredda M L, Ammendola S, Sciammarella C, et al. Colorectal cancer with microsatellite instability: Right-sided location and signet ring cell histology are associated with nodal metastases, and extranodal extension influences disease-free survival[J]. Pathology, Research and Practice, 2021, 224(153519.
16. Fan S, Li X, Cui X, et al. Computed Tomography-Based Radiomic Features Could Potentially Predict Microsatellite Instability Status in Stage II Colorectal Cancer: A Preliminary Study[J]. Academic

Radiology, 2019, 26(12):1633-1640.
17. Shu Z, Mao D, Song Q, et al. Multiparameter MRI-based radiomics for preoperative prediction of extramural venous invasion in rectal cancer[J]. European Radiology, 2021.
18. Zhang W, Yin H, Huang Z, et al. Development and validation of MRI-based deep learning models for prediction of microsatellite instability in rectal cancer[J]. Cancer Med, 2021, 10(12):4164-4173.
19. Shayesteh S, Nazari M, Salahshour A, et al. Treatment response prediction using MRI-based pre-, post-, and delta-radiomic features and machine learning algorithms in colorectal cancer[J]. Medical Physics, 2021, 48(7):3691-3701.
20. Kloor M, Staffa L, Ahadova A, et al. Clinical significance of microsatellite instability in colorectal cancer[J]. Langenbeck's Archives of Surgery, 2014, 399(1):23-31.

Figures

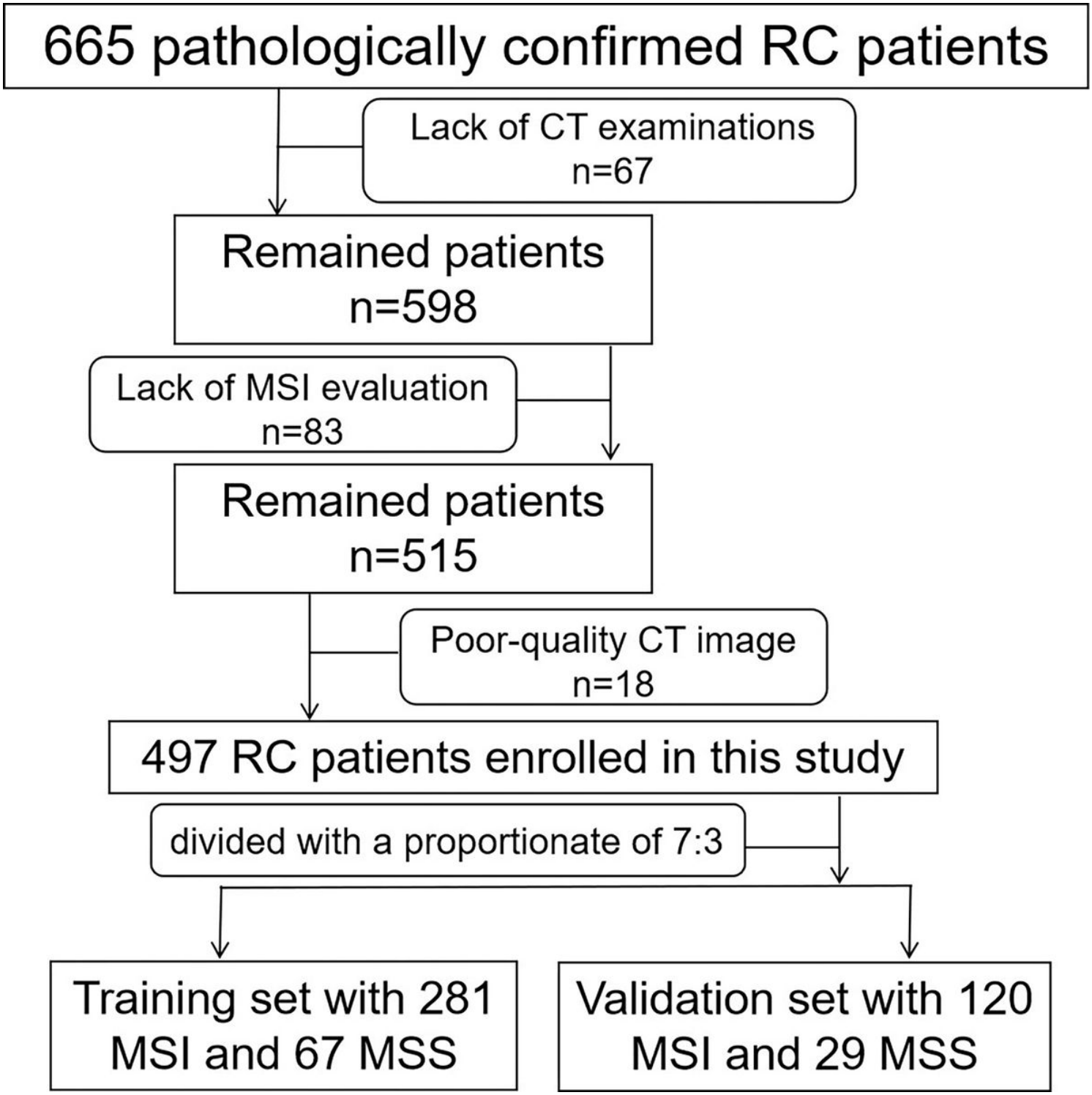

Figure 1

The flow-chat of patient selection.

Figure 2

The VOI-t was manually depicted in the itk-SNAP software (2a). The VOI-pt was delineated after expanding 5mm from the margin of tumor, automatically (2b).

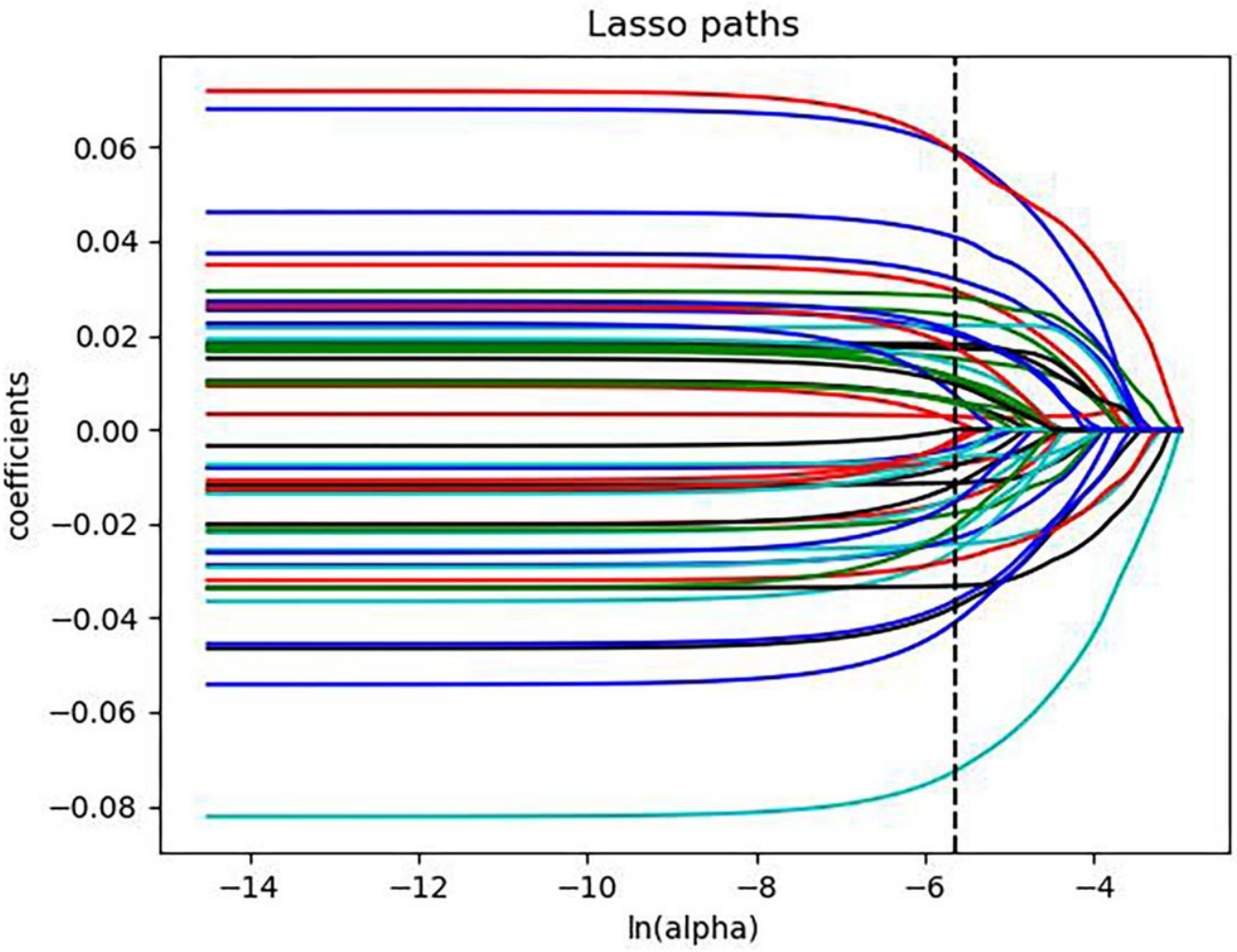

Figure 3

The LASSO path plot of the M-LR in the training set. After the dimension reduction method of LASSO, there were 51 radiomic features left.

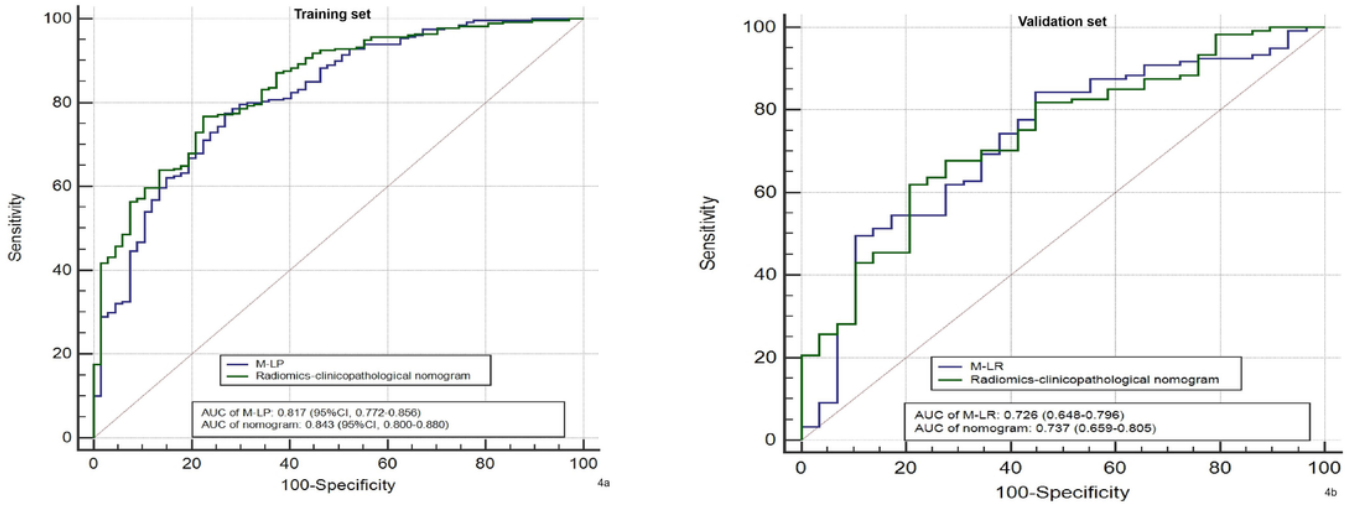

Figure 4

The comparison of AUCs in M-LR and radiomics-clinicopathological nomogram in the training set and validation set. The AUCs of radiomics-clinicopathological were higher in the training and validation set than those of M-LR.

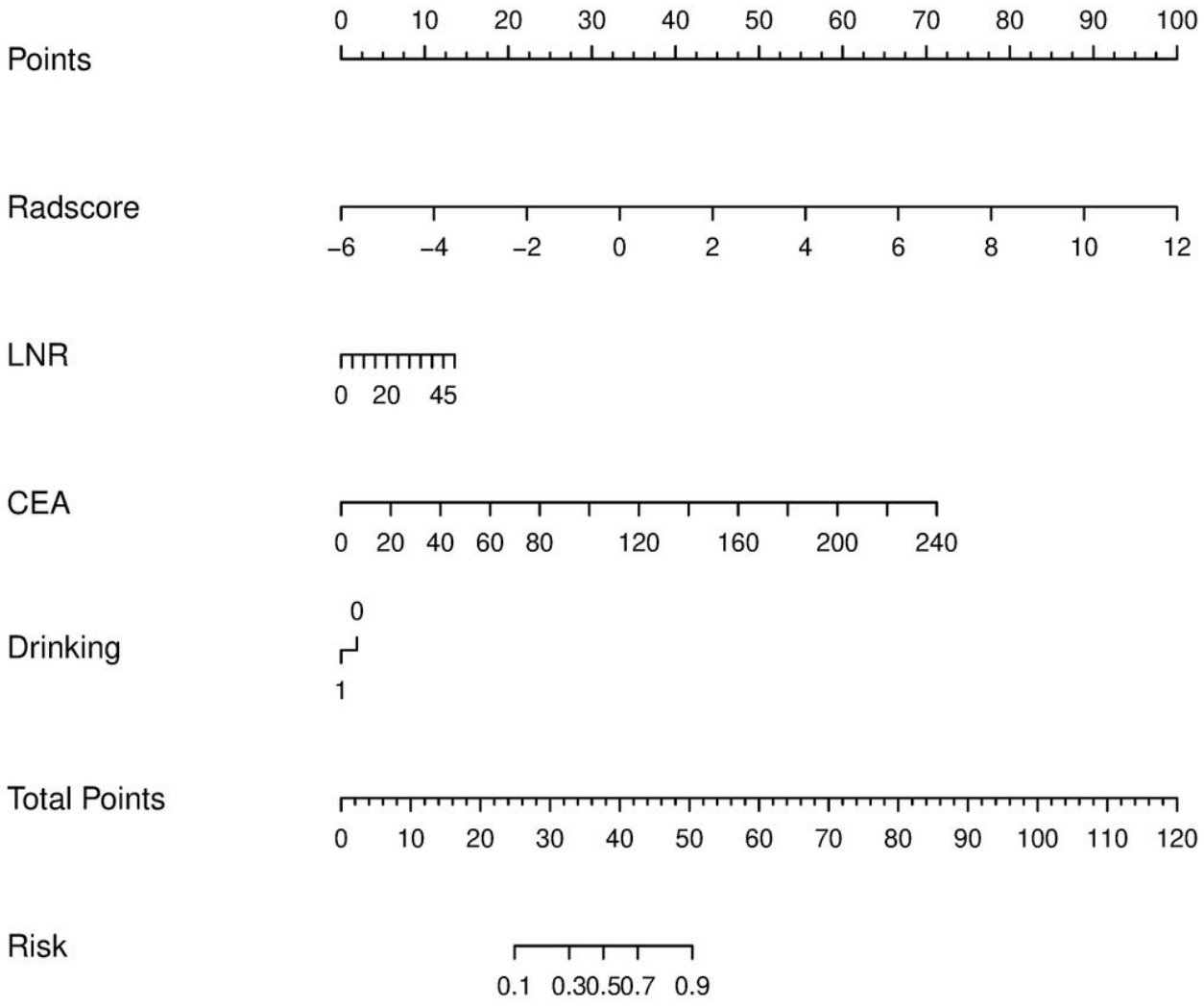

Figure 5

The radiomics-clinicopathological nomogram including Rad-score and significant clinicopathological characteristics of CEA, LNR, and drinking history.

Supplementary Files

This is a list of supplementary files associated with this preprint. Click to download.

- SupplementMaterial.doc